energies

MDPI

Article

Combustion Characterization and Kinetic Analysis of Coupled Combustion of Bio-Syngas and Bituminous Coal

Ailing He [1], Zaifeng Li [2], Bingdong Gu [1] and Tingzhou Lei [3,*]

[1] School of Civil and Transportation Engineering, Qinghai Minzu University, Xining 810007, China; heailing1110@163.com
[2] Henan Key Lab of Biomass Energy, Zhengzhou 450008, China
[3] Institute of Urban & Rural Mining CCZU, Changzhou University, Changzhou 213164, China
* Correspondence: china_newenergy@163.com

Abstract: The coupled combustion of bio-syngas and bituminous coal is an effective technology to reduce pollutant emissions from coal-fired power plants and improve the utilization rate of biomass energy. However, the effects of bio-syngas blending on bituminous coal combustion characteristics and reaction kinetics remain unclear, restricting the development of bio-syngas and bituminous coal combustion technology. In this study, the experimental studies on the coupled combustion of bio-syngas and bituminous coal under different bio-syngas lower-heating-value-based blending ratio (BLBR) were carried out by Micro-Fluidized Bed Reaction Analyzer (MFBRA), the coupled combustion characteristics and kinetic reaction mechanism of coupled combustion of bio-syngas and bituminous coal were analyzed. The results indicated that the nucleation and growth model (F1 Model) provided a reasonable description of the bituminous coal combustion process on the coupled combustion of bio-syngas and bituminous coal in MFBRA. The blending of bio-syngas significantly reduces the apparent activation energy and pre-exponential factor of bituminous coal combustion reaction. In particular, when the BLBR is 5, 10, 20, and 30%, the apparent activation energy is 48.70, 45.45, 46.75, and 42.35 kJ·mol^{-1}, and the pre-exponential factor is 9.26, 7.10, 8.95, and 6.70 s^{-1}, respectively. This research is helpful for improving the coupled combustion efficiency and ensuring the efficient operation of the coupled combustion system.

Keywords: coupled combustion; micro-fluidized bed reaction analyzer; bio-syngas; bituminous coal; reaction mechanism; bio-syngas lower heating value-based blending ratio (BLBR)

check for updates

Citation: He, A.; Li, Z.; Gu, B.; Lei, T. Combustion Characterization and Kinetic Analysis of Coupled Combustion of Bio-Syngas and Bituminous Coal. *Energies* **2024**, *17*, 6205. https://doi.org/10.3390/en17236205

Academic Editor: Fernando Rubiera González

Received: 9 November 2024
Revised: 2 December 2024
Accepted: 8 December 2024
Published: 9 December 2024

Copyright: © 2024 by the authors. Licensee MDPI, Basel, Switzerland. This article is an open access article distributed under the terms and conditions of the Creative Commons Attribution (CC BY) license (https://creativecommons.org/licenses/by/4.0/).

1. Introduction

As the social economy continues to develop and CO_2 is continuously emitted, the global warming caused by the greenhouse effect is endangering the eco-system. Therefore, in order to tackle global climate change, a temperature control target of 1.5 °C has been set at the global level; meanwhile, over 130 countries and regions have set carbon-neutral targets [1]. China, as the largest emitter of anthropogenic CO_2 [2,3], announced that it is committed to reaching the carbon peak by 2030 and achieving carbon neutrality by 2060 in September 2020. With these targets in place, the coal power industry, which is the largest emitter of anthropogenic CO_2 emissions, will need to strengthen its actions to curb emissions [4].

At present, coal consumption still remains the principal energy consumption resource in China [5]. According to the Annual Development Report of Power Industry for China 2024, at the end of 2023, China's total power generation installed capacity was 292.224 million kilowatt hours, and the installed capacity of coal-fired power generation was 139.099 million kilowatt hours, accounting for 47.6% of the total power generation installed capacity. This indicates that coal is still the largest energy consumption resource in the power industry. In accordance with the Statistical Review of World Energy, global coal consumption increased by 1.6% in 2022, and coal continues to be the dominant energy

consumption resource in power generation, with a stable share of approximately 35% in 2023. In conclusion, the power industry urgently requires the exploration of clean energy resources to partially substitute coal, aiming to mitigate the issues brought about by the copious CO_2 emissions resulting from coal combustion [6,7]. Globally and within China alike, bituminous coal distinguishes itself with the broadest distribution, the most substantial reserves, and the most prevalent utilization in the power sector. Additionally, bituminous coal exhibits a comparatively high calorific value and a stable combustion characteristic. Consequently, the clean utilization of bituminous coal is of greater significance. Among the technologies for reducing emissions from coal-fired power plants, the coupled combustion power generation technology of biomass and coal, as one of the most efficient and economical approaches, can partially replace coal consumption for power generation, thus curbing carbon dioxide emissions from coal-fired power plants [8–10]. Furthermore, biomass exhibits characteristics such as renewability, low carbon emissions, versatility, local availability, and waste reduction. Consequently, biomass is considered one of the best alternative resources for power plants.

Bio-syngas, produced by the air gasification of biomass, is mainly composed of carbon monoxide (CO), methane (CH_4), and hydrogen (H_2) [11,12]. The coupled combustion of bio-syngas and coal, an indirect coupled combustion technology for biomass and coal, offers advantages such as wide fuel adaptability, a high biomass blending ratio, and prevention of boiler slagging and corrosion [13,14]. It can make use of existing large and expensive infrastructure; however, the stability and thermal efficiency of the original coal-fired unit may be influenced by the blending of bio-syngas [15].

In the coupled combustion of bio-syngas and coal, there exist multiple complex physical and chemical processes, including the drying of coal particles, the release and combustion of volatile matter, the combustion of coke, and the combustion of bio-syngas [16,17]. For coal combustion, the blending of bio-syngas acts as a combustion-supporting role, enabling coal to burn more thoroughly; meanwhile, coal combustion also enhances the stability of bio-syngas combustion. Thus, in the coupled combustion process, the combustion of bio-syngas and that of coal influence each other. For now, scholars have carried out extensive research on the release characteristics of volatile matter and combustion mechanisms of coal particles in different atmospheres [18–20]. By conducting research on the ignition behavior of a single coal particle in a fluidized bed in O_2/CO_2 and O_2/N_2 atmospheres, it was indicated that the ignition delay time in the O_2/CO_2 atmosphere is significantly longer than that in the O_2/N_2 atmosphere [21]. Zhang et al. [22] revealed the homogeneous ignition mechanism of coal in O_2/CO_2 atmospheres and the reasons for the ignition delay compared to the corresponding O_2/N_2 atmosphere. Based on the isothermal thermal analysis method, Lei et al. [23] investigated the combustion characteristics of pulverized coal in different atmospheres (O_2/N_2, O_2/CO_2, and $O_2/H_2O/CO_2$). Their results indicated that the impact of CO_2 and H_2O gasification is enhanced as the temperature rises at a low oxygen concentration, and the coal burning rate in $O_2/H_2O/CO_2$ is higher than that in O_2/CO_2. The blending of bio-syngas has an effect on all stages of the coal combustion process, thereby changing the combustion characteristics of coal. More research work has been conducted on the burnout characteristics and NOx of coupled combustion of bio-syngas and coal [24–27]. The results indicate that upon blending high-coal furnace gas, the average residence time of flue gas is decreased, it is difficult for the coal in the furnace to be completely burned out, and the furnace temperature is lowered. Ye et al. [28] proposed a calculating model to calculate the thermal efficiency of pulverized coal and blast furnace gas co-fired boilers. However, there are relatively few reports available on the combustion kinetics characteristics in a multiple mixed atmosphere, as well as on the coupled combustion mechanism of bio-syngas and coal. Therefore, deeper exploration of the coupled combustion mechanism of bio-syngas and coal holds significant theoretical and practical importance for enhancing combustion efficiency and controlling pollution emissions.

The main experimental research for the kinetics and reaction features of coal combustion comprises the Micro-Fluidized Bed Reaction Analyzer (MFBRA) [29–31], thermogravimetric

analyzer (TGA) [32–34], Drop Dube Furnace (DDF) [35,36], and laser diagnostic technology [37]. MFBRA, an isothermal analysis method, has the characteristics of high heating rate, on-line feed and measuring the gas product, and minimized diffusion inhibition. Thereby, compared with the TGA method, the MFBRA method has been widely utilized in the research on combustion characteristics and the calculation of kinetic parameters, and also applied to determine the underlying mechanism. The kinetics mechanism of coal pyrolysis and coal char combustion have been studied using an MFBRA [38–40]. In terms of the coal combustion mechanism, there are mainly two cases. Firstly, in comparison with the combustion rate of coal char, the combustion rate of volatile matter can be ignored. Secondly, pyrolysis and coal char combustion are two separate processes. There is limited research on the entire combustion process, especially in terms of the kinetic mechanism [41,42].

In this work, the coupled combustion characteristics and mechanism of bio-syngas and bituminous coal will be investigated by the MFBRA method. The release characteristic of gas products during the coupled combustion process with four bio-syngas lower heating value-based blending ratios (BLBRs) and under five temperatures will be discussed. The combustion mechanisms of bituminous coal particles in coupled combustion will be thoroughly investigated. Furthermore, the influence of BLBR on the kinetic parameters of bituminous coal particle combustion during coupled combustion will be clarified.

2. Materials and Methods

2.1. Raw Material Properties

The bituminous coal (BC) and bio-syngas (BS) were selected as the raw materials for coupled combustion in the present study. Bituminous coal samples were collected from Pingdingshan City, Henan Province, China, and ground using a coal mill. Then, the bituminous coal with a particle size ranging from 60 to 100 mesh was obtained by screening. The results of proximate and ultimate analysis, as well as the lower heating value (LHV) of the bituminous coal, are given in Table 1. Bio-syngas samples were compounded by Henan Yuan zheng Special Gas Co., Ltd., Zhengzhou City, Henan Province, China. The composition of the bio-syngas, which consists of CO, CH_4, H_2, CO_2, and N_2, is given in Table 2, and the main combustible constituents of the bio-syngas were CO, H_2, and CH_4. Bio-syngas is formulated according to the components of the products of the air gasification of biomass at 800 °C. High-purity quartz sand samples (SiO_2 > 99.8%) were purchased from Qinghe County Tuopu Material Co., Ltd., Xingtai City, Hebei Province, China.

Table 1. Proximate and ultimate analysis for bituminous coal (wt%, air-dry basis).

Materials	Proximate Analysis				Ultimate Analysis					LHV_{BC}
	V	FC [c]	A	M	C	H	N	S	O [c]	kJ/kg
Bituminous coal	29.91	57.51	5.41	7.17	68.31	5.62	0.72	0.83	11.94	25228

[c] Calculated by mass balance.

Table 2. The composition, lower heating value, and density of bio-syngas.

	CO/%	CO_2/%	H_2/%	N_2 [c]/%	CH4/%	ρ [c]/(kg/m^3)	LHV_{BS} [c]/(kJ/m^3)
Bio-syngas	21.99	13.01	14.01	48.99	2.00	1.17	5003

[c] Calculation result.

2.2. Experimental Apparatus

The coupled combustion experiments of bio-syngas and bituminous coal were performed in MFBRA, which mainly includes components such as corundum reactor, perforated plates, air compressors, bio-syngas cylinders, pulse injectors, filters, online mass spectrometer (GSD 320, Pfeiffer Vacuum, Asslar, Germany, the error of 30% (on the order of ppm)), valves, pressure gauges, mass flow meters, and temperature controllers, as shown in Figure 1. The corundum reactor is heated by a 30 kW microwave radiation heating

furnace, and the maximum temperature can reach 1400 °C. The outside and inner diameter of the corundum reactor are 0.026 m and 0.019 m, the total length is 0.52 m, and a porous plate is placed in the interior of the corundum reactor. The quartz sand bed material with a mean diameter of 1.25×10^{-4} m is placed in the porous plate, and the loading height is 0.030 m. Five branches were designed in the corundum reactor, the first one for solid particle injection by compressed air, the second for temperature sensors' installation, the third for the inflow of compressed air, the fourth for the inflow of bio-syngas, and the last for process mass spectrometry bonding. The flow rates of the compressed air and bio-syngas were controlled using two-mass flowmeter. Compressed air and quartz sand were used as the carrier gas and the fluidization medium, respectively. The flow rate of the carrier gas, temperature of the furnace, and actions of pulse sample injection were all controlled by a computer.

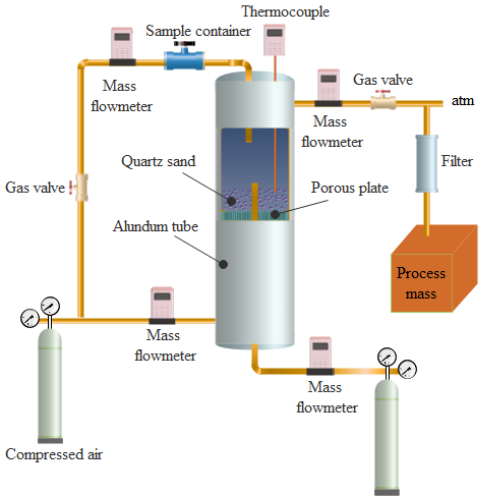


Figure 1. Schematic diagram of the MFBRA for the coupled combustion of bio-syngas and bituminous coal.

2.3. Experimental Setup

In this experiment, for the purpose of studying the kinetic law of the coupled combustion of bio-syngas and bituminous coal, an online mass spectrometer was used to characterize the coupled combustion process of bio-syngas and bituminous coal. The coupled combustion experiments were performed at four *BLBRs* (5%, 10%, 20%, and 30%) and five temperatures (873 K, 973 K, 1073 K, 1173 K, and 1273 K). According to the LHV_{BC} and LHV_{BS} listed in Tables 1 and 2, the BLBR of each group was calculated as follows [43]:

$$BLBR = \frac{LHV_{BS} \cdot t \cdot q_{V,BS}}{LHV_{BS} \cdot t \cdot q_{V,BS} + LHV_{BC} \cdot m_{BC}} \quad (1)$$

where *BLBR* represents the bio-syngas lower heating value-based blending ratio in coupled combustion experiments, %; LHV_{BS} denotes the lower heating value of bio-syngas, kJ·m^{-3}; LHV_{BC} is the lower heating value of bituminous coal, kJ·kg^{-1}; t denotes the bio-syngas entry time, s; $q_{V,BS}$ is the volume flow rate of bio-syngas, sccm; and m_{BC} denotes the mass of bituminous coal, kg.

Before the beginning of each experiment, five temperature ranges (from room temperature to 873 K, 973 K, 1073 K, 1173 K, and 1273 K) were set in the same atmosphere by the microwave radiation heating furnace. Air was introduced into the reactor, and then the quartz sand particles in the reactor were kept in a steadily fluidized state. The bio-syngas with a set flow rate (flow rate: 1.7 sccm, 3.7 sccm, 8.4 sccm, and 16 sccm) flows into the reactor. Then, bituminous coal samples with a mass of about 10 mg were injected into the hot quartz sand particles to cause rapid mixing and reaction. The flue gas (CO, CO_2, O_2, and N_2) was monitored online using a mass spectrometer on a continuous basis. The

reaction characteristics and kinetic mechanism were analyzed based on the release features of gas components given by the online mass spectrometry.

2.4. Model Description

Widely used kinetic mechanism functions of solid-state combustion are listed in Table 3. In this study, it was assumed that the release and combustion of volatile fraction and the combustion of coal char occurred simultaneously, and the combustion of coal char plays a dominant role in the combustion of bituminous coal, which determines the combustion time and completeness of bituminous coal. Due to the use of the high temperatures and the small size of the coal particles, the interconnected processes of volatile release and combustion, along with coal char combustion, collectively influence and determine the overall reaction rate of bituminous coal combustion. So, the total reaction mechanism of bituminous coal combustion can be expressed by Equation (2):

$$\text{Coal} + O_2 \rightarrow H_2O + CO_2 + CO + \text{Ash} \quad (2)$$

Table 3. Widely used kinetic mechanism functions of solid-state combustion [40–42].

Model	Mechanism	$f(\alpha)$	$G(\alpha)$
1	One-dimensional diffusion, 1D	$1/2\alpha$	α^2
2	Zero order, F0/R1	1	α
3	First order, F1	$1-\alpha$	$-ln(1-\alpha)$
4	Second order, F2	$(1-\alpha)^2$	$(1-\alpha)^{-1}-1$
5	Third order, F3	$(1-\alpha)^3$	$\frac{1}{2}\left[(1-\alpha)^{-2}-1\right]$
6	Four order, F4	$(1-\alpha)^4$	$\frac{1}{3}\left[(1-\alpha)^{-3}-1\right]$
7	Contracting area, R2	$2(1-\alpha)^{1/2}$	$1-(1-\alpha)^{1/2}$
8	Contracting volume, R3	$3(1-\alpha)^{2/3}$	$1-(1-\alpha)^{1/3}$
9	Nucleation and growth	$\frac{2}{3}(1-\alpha)[-ln(1-\alpha)]^{1/3}$	$[-ln(1-\alpha)]^{2/3}$
10	Nucleation and growth, A2	$2(1-\alpha)[-ln(1-\alpha)]^{1/2}$	$[-ln(1-\alpha)]^{1/2}$
11	Nucleation and growth, A3	$3(1-\alpha)[-ln(1-\alpha)]^{2/3}$	$[-ln(1-\alpha)]^{1/3}$
12	Nucleation and growth, A4	$4(1-\alpha)[-ln(1-\alpha)]^{3/4}$	$[-ln(1-\alpha)]^{1/4}$
13	One-dimensional diffusion, D1	$\frac{\alpha}{2}$	α^2
14	Two-dimensional diffusion, D2	$[-ln(1-\alpha)]^{-1}$	$\alpha+(1-\alpha)ln(1-\alpha)$
15	Shrinkage geometrical, P2	$2\alpha^{1/2}$	$\alpha^{1/2}$
16	Shrinkage geometrical, P3	$3\alpha^{2/3}$	$\alpha^{1/3}$
17	Shrinkage geometrical, P4	$4\alpha^{3/4}$	$\alpha^{1/4}$

2.5. Computational Theory of Kinetic Parameters

The combustion of coal can be described as a single-step kinetic equation with temperature (T) and carbon conversion rate (α). In this work, based on the release characteristics of CO and CO_2 measured at different reaction temperatures (from 873 to 1273 K) and BLBR, the combustion kinetics of coal were analyzed in the coupled combustion of bio-syngas and coal. The conversion rate (α) and combustion reaction rate (v) of coal in the coupled combustion of bio-syngas and coal can be expressed by the following:

$$\alpha = \frac{\int_{t_0}^{t} \left(\varphi_{CO} + \varphi_{CO_2}\right) \times u dt}{\int_{t_0}^{t_\infty} \left(\varphi_{CO} + \varphi_{CO_2}\right) \times u dt} \quad (3)$$

$$v = \frac{d\alpha}{dt} \quad (4)$$

where α is the conversion rate of coal in the coupled combustion of bio-syngas and coal, %; φ_{CO} is the volume fraction of the CO component in flue gas, %; φ_{CO_2} represents the volume fraction of the CO_2 component in flue gas, %; u denotes the volume rate of all

gas components, $m^3 \cdot s^{-1}$; t_0 and t_∞ represent the initial time and end time of the coupled combustion reaction, respectively, s; t is the duration of coupled combustion reaction, s; and v is the combustion reaction rate of coal in the coupled combustion of bio-syngas and coal, s^{-1}. According to the gas release characteristics of CO and CO_2 in the coupled combustion process of bio-syngas and coal, the release of CO is very little, and the oxygen consumption rate is approximately equal to the carbon release rate. Therefore, in the analysis process, it is assumed that the flue gas volume is equal to the sum of the bio-syngas volume and the fluidized gas volume.

(1) Basic kinetic equation

The basic kinetic equations of heterogeneous reaction under isothermal conditions are represented by the following:

$$\frac{d\alpha}{dt} = k(T) \times f(\alpha) \tag{5}$$

$$G(\alpha) = \int_0^\alpha \frac{d\alpha}{f(\alpha)} \tag{6}$$

where $f(\alpha)$ is the differential format of basic kinetic equation; $G(\alpha)$ denotes the integral format of basic kinetic equation; T is the temperature of combustion reaction, K; and $k(T)$ is the reaction rate constant at reaction temperature T, s^{-1}.

According to the Arrhenius law, the reaction rate constant can be expressed by the following:

$$k(T) = Aexp\left(-\frac{E}{RT}\right) \tag{7}$$

where A denotes the pre-exponential factor, s^{-1}; E denotes the apparent activation energy, $J \cdot mol^{-1}$; and R is the ideal gas constant, 8.314 $J \cdot (mol\ K)^{-1}$.

By combing Equations (5) and (7), we obtain the following:

$$\frac{d\alpha}{dt} = Aexp\left(-\frac{E}{RT}\right) f(\alpha) \tag{8}$$

By substituting Equation (8) into Equation (6), we obtain the following:

$$G(\alpha) = k(T) \times t \tag{9}$$

(2) Kinetic mechanism model function

Firstly, according to Equation (9), the data pertaining to $G(\alpha)$ versus t at different temperatures can be fitted as a straight line, and $k(T)$ can be represented by the slope. In this work, four types of reaction mechanism model functions were applied, and the best reaction mechanism model function was selected based on the goodness of fit (R^2) and standard deviation (SD). Secondly, taking the logarithm of both sides of Equation (7), we obtain the following:

$$lnk(T) = -\frac{E}{RT} + lnA \tag{10}$$

According to Equation (10), the data pertaining to $lnk\ (T)$ versus $1/T$ can be fitted as a straight line, and the apparent activation energy and pre-exponential factor are calculated by the intercept and slope of the line.

(3) Iso-conversional rate method

Taking the logarithm of both sides of Equation (8), we obtain the following:

$$ln\frac{d\alpha}{dt} = -\frac{E}{RT} + lnA + lnf(\alpha) \tag{11}$$

According to Equation (11), the relationship between $ln(d\alpha/dt)$ and $1/T$ can be fitted as a straight line under iso-conversion rate conditions. The apparent activation energy can be calculated based on the slope of the straight line.

Finally, the best reaction mechanism model function is determined by the linearity of the relationship between the reaction mechanism model function and time, and the approximation degree of calculating the reaction activation energy by the iso-conversion-rate method and the model fitting method, and the kinetic parameters are determined.

3. Results and Discussion

3.1. Combustion Characteristics and Factors

In this work, the coupled combustion experiments of bio-syngas and bituminous coal with four *BLBRs* (5%, 10%, 20%, and 30%) were performed at 873 K, 973 K, 1073 K, 1173 K, and 1273 K in the MFBRA, respectively. The concentrations of CO and CO_2 gas production of the coupled combustion experiments of bio-syngas and bituminous coal are shown in Figures 2 and 3, obtained using a mass spectrometer.

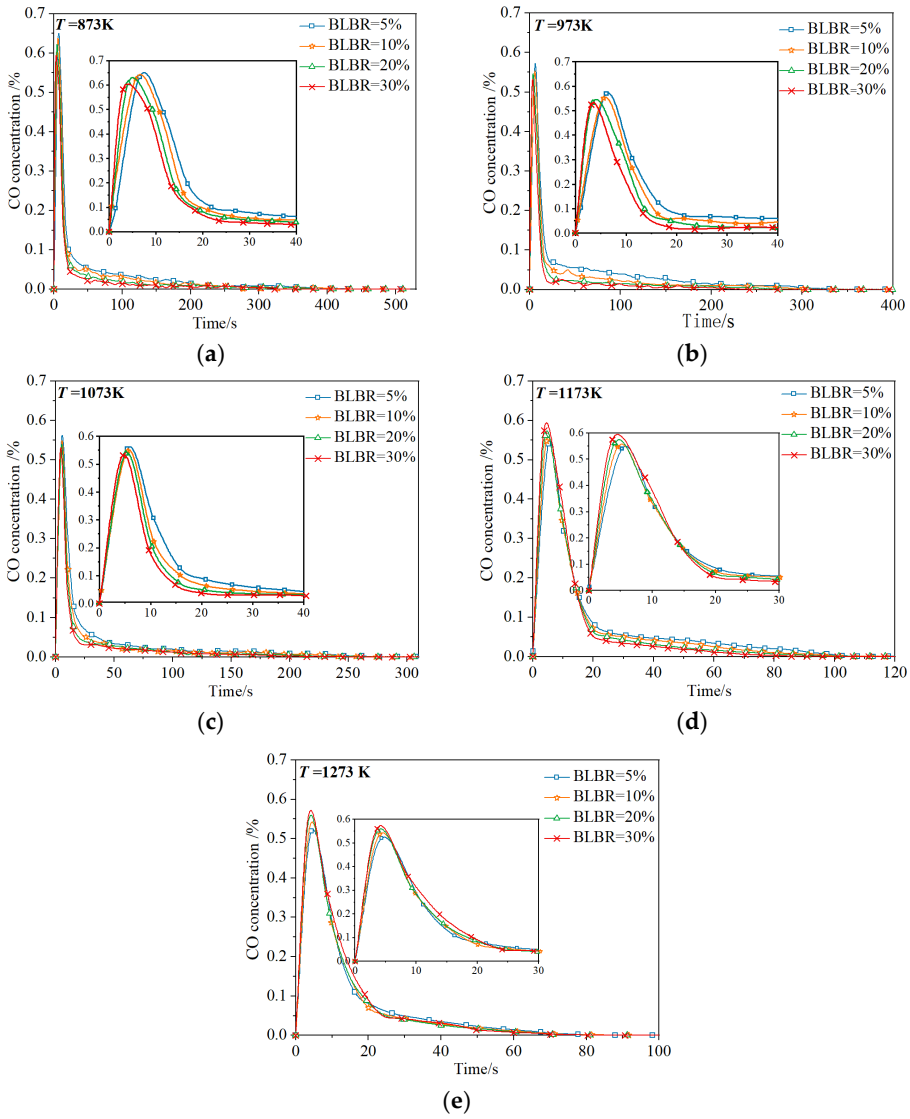


Figure 2. Concentrations of CO gas production versus time at the coupled combustion of bio-syngas and bituminous coal. (**a**) $T = 873$ K, $BLBR = 5 \sim 30\%$; (**b**) $T = 973$ K, $BLBR = 5 \sim 30\%$; (**c**) $T = 1073$ K, $BLBR = 5 \sim 30\%$; (**d**) $T = 1173$ K, $BLBR = 5 \sim 30\%$; (**e**) $T = 1273$ K, $BLBR = 5 \sim 30\%$.

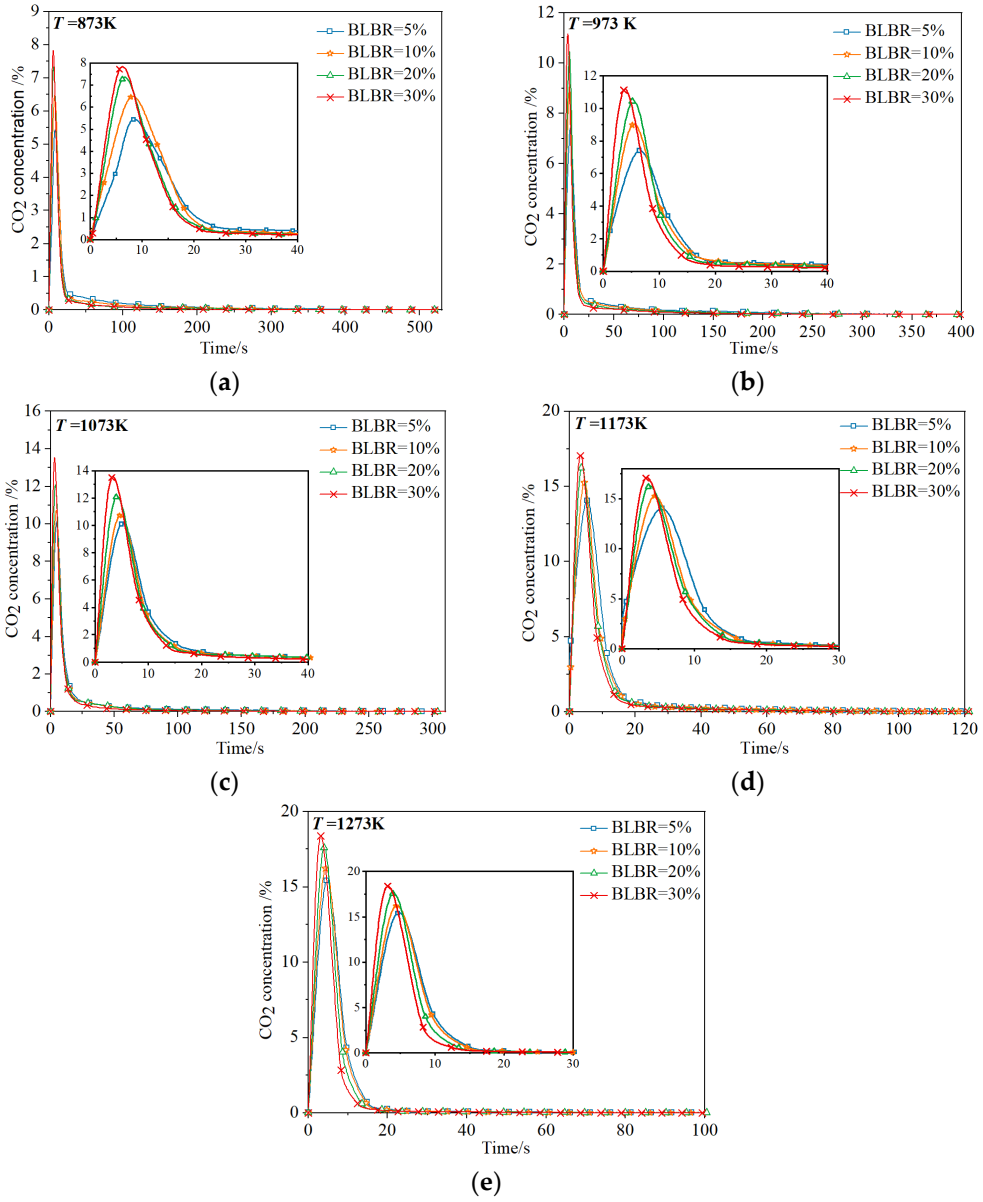


Figure 3. Concentrations of CO_2 gas production versus time at the coupled combustion of bio-syngas and bituminous coal. (**a**) $T = 873$ K, $BLBR = 5 \sim 30\%$; (**b**) $T = 973$ K, $BLBR = 5 \sim 30\%$; (**c**) $T = 1073$ K, $BLBR = 5 \sim 30\%$; (**d**) $T = 1173$ K, $BLBR = 5 \sim 30\%$; (**e**) $T = 1273$ K, $BLBR = 5 \sim 30\%$.

3.1.1. Effect of Temperature on Gas Production

Based on Figures 2 and 3, with the increase in temperature, the release trend of CO and CO_2 gas products appears to be consistent, showing a trend of increasing first and then decreasing. The completion time of the main combustion reaction ranges from 10 to 25 s, and the peaks of CO and CO_2 concentrations both appear within the range from 2 to 8.5 s after the start of combustion. The main reason is that the heating rate of bituminous coal and bio-syngas is relatively high under isothermal conditions; the processes, such as moisture removal, release and combustion of volatile fraction, and combustion of coal char, take place almost simultaneously and go on in an intersecting manner, and the CO and CO_2 is rapidly released [44]. As the reaction proceeds, the combustible substances continuously react with oxygen, and the concentrations of CO and CO_2 rapidly drop and gradually become zero. At the same time, it can also be seen from Figures 2 and 3 that in comparison with the concentration of CO_2, the amount of CO is extremely small. This

is mainly due to the fact that the excess air coefficient is relatively large in the coupled combustion process and the reaction rate of CO conversion to CO_2 is accelerated in the presence of hydrogen.

3.1.2. Effect of BLBR on Gas Production

As can be seen from Figures 2 and 3, it was demonstrated that the influence of BLBR on the concentrations CO and CO_2 gas production in the coupled combustion process was inconsistent at different temperatures, and the time to completion of the reaction was shortened with the increase in BLBR from 5% to 30%. At 873–1073 K, as the BLBR increases, the concentration of CO gas production decreases, the concentration of CO_2 increases, and the release curves of CO and CO_2 gas production shift to the left. The reasons why are mainly as follows: On the one hand, the greater the BLBR, the higher the content of combustible components, thus accelerating the release and combustion of volatile fraction, and the ignition and combustion of coal char. Moreover, the hydrogen contained in bio-syngas and bituminous coal greatly accelerates the reaction rate of CO converting to CO_2. On the other hand, within the range of 873–1073 K, the gasification reaction of coal char has not occurred yet. At 1173–1273 K, the concentrations of CO and CO_2 both increase with the increase in the BLBR, mainly due to the increase in the BLBR, which promotes the gasification reaction of coal char and thereby increases the concentrations of CO.

3.1.3. Coupled Combustion Characteristics

According to Equation (3), the relationship between carbon conversion and time is illustrated in Figure 4a,b. Figure 4a shows that carbon conversion of bituminous coal increased slightly, and the burnout time decreased with the increase in BLBR. The major carbon conversion process (90%) can be completed within 18 s at $T = 1173$ K and $BLBR = 30\%$. Based on Figure 4b, as the temperature was increased from 873 K to 1273 K, carbon conversion of bituminous coal increased quickly in the initial stage, and the major reaction process and the burnout time were shortened. The major carbon conversion process (90%) can be completed within 15 s at $T = 1273$ K and $BLBR = 10\%$, which is much shorter compared with the reaction equilibrium time.

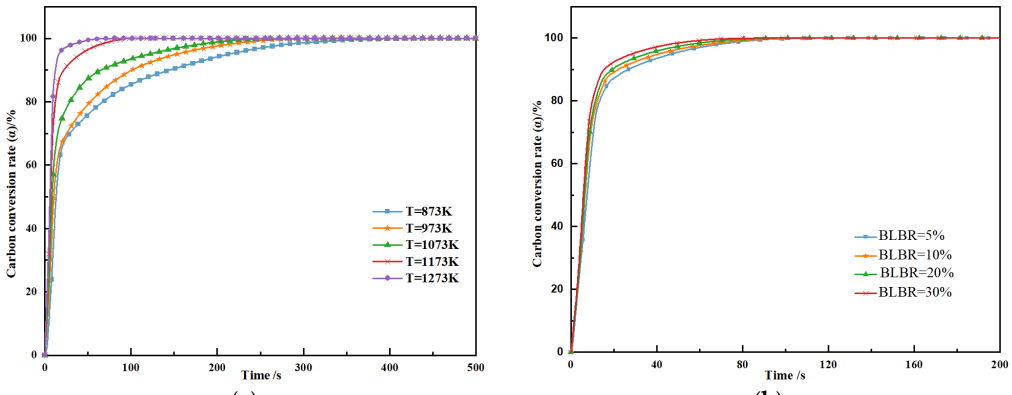


Figure 4. Linear fitting relationship diagram of $lnk(T)$ and $1000/T$. (**a**) $T = 1173\ K$, $f_{bio}^{cvb} = 5 \sim 30\%$; (**b**) $T = 873 \sim 1273\ K$, $f_{bio}^{cvb} = 10\%$.

3.2. Kinetic Analysis of Bituminous Coal in Coupled Combustion

In this study, the iso-conversional method and the model-fitting method are adopted to investigate the kinetic mechanism of bituminous coal in coupled combustion of coupled combustion.

3.2.1. Iso-Conversional Method

According to Equation (4), the relationship between the rate of bituminous coal combustion reaction and carbon conversion, α, is illustrated in Figure 5 at $BLBR = 10\%$ within

the temperature range of 873~1273 K. Figure 5 shows that the rate of bituminous coal combustion reaction in the temperature range of 873~1273 K presents a trend of first increasing and then decreasing with the increase in the carbon conversion rate. The position where the highest combustion reaction rate appears shifts to the right, and the main combustion reaction process is between $\alpha = 0.2$ and $\alpha = 0.90$. This is mainly because bituminous coal combustion belongs to the diffusion combustion at high temperatures.

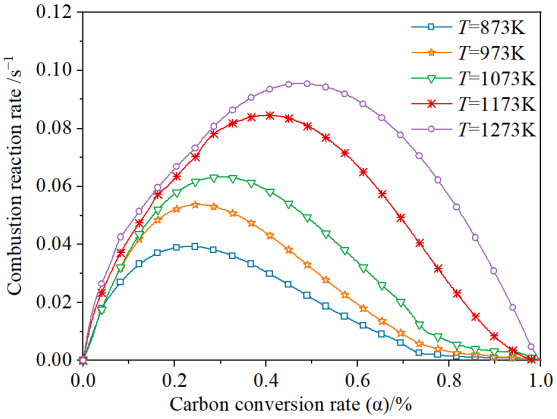


Figure 5. Combustion rate of bituminous coal versus carbon conversion, α ($BLBR = 10\%$).

On the basis of the data shown in Figure 5, a good linear relationship between $ln\ (d\alpha/dt)$ and $1000/T$ was fitted under different carbon conversion, as shown in Figure 6. The results of linear fitting and the apparent activation energy are shown in Table 4; moreover, the goodness of fit (R^2) of each fitting curve is greater than 0.9. As shown in Table 4, as the conversion rate increases from 0.1 to 0.9, the apparent activation energy varies within the range from 20.54 to 78.54 kJ·mol^{-1}. Taking the average value of the apparent activation energy between conversion rates of 0.1 and 0.9, the apparent activation energy of bituminous coal combustion is 44.88 kJ·mol^{-1}.

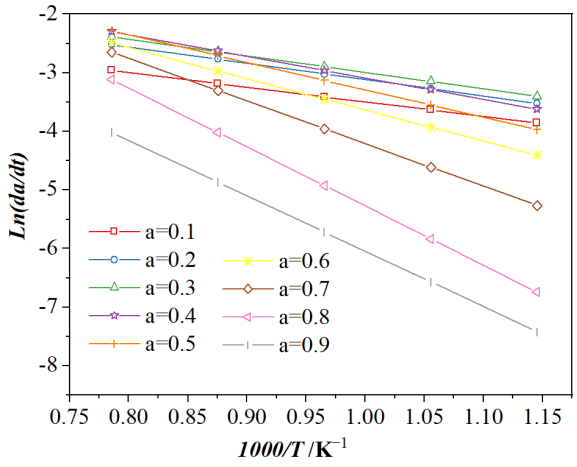


Figure 6. Linear fitting relationship diagram of $ln(d\alpha/dt)$ and $1000/T$.

Table 4. Apparent activation energies of the bituminous coal combustion (kJ·mol^{-1}, 873–1273 K).

	0.10	0.20	0.30	0.40	0.50	0.60	0.70	0.80	0.90	Average Value
E	20.54	23.32	23.45	30.71	38.83	44.27	60.47	83.80	78.54	44.88
R^2	0.9709	0.9904	0.9565	0.9405	0.9448	0.9176	0.9014	0.9470	0.9000	
SD	0.2069	0.2933	0.0851	0.1312	0.1595	0.2247	0.3381	0.3372	0.4432	

3.2.2. Model-Fitting Method

Based on the characteristics of bituminous coal combustion reaction, five mechanism function models (F0 Model, R2 Model, R3 Model, F1 Model, and A2 Model) of Table 3 are selected for kinetics analysis of bituminous coal combustion reaction in coupled combustion. In accordance with Equation (9), the rate constant of combustion reaction $k(T)$ is derived from the correlation between the function models, G(a), and the reaction time, t (Figure 7). The shapes of the fitting curves differ significantly, and the F0 Model, R2 Model, and R3 Model all have a relatively wide linear range in the low-temperature zone; nevertheless, there is a linear partition in the high-temperature region, indicating that the F0 Model, R2 Model, and R3 Model may not be consistent with the actual reaction mechanism. For the F1 Model and the A2 Model, the shapes of the G(a) curves are similar. However, the F1 Model exhibits excellent linearity in the main reaction process and has a relatively wide linear range.

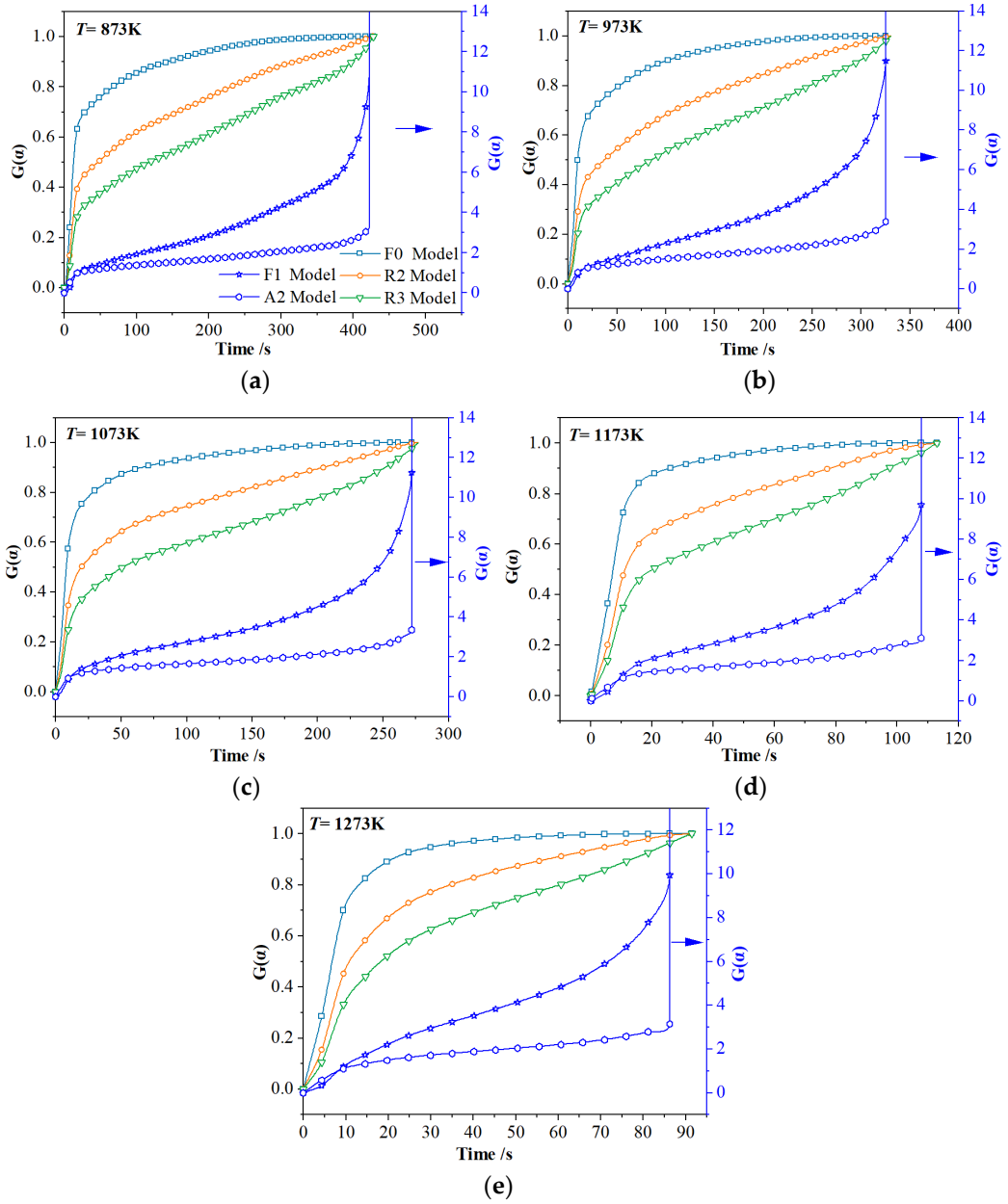


Figure 7. Mechanism function models versus reaction time. (**a**) $T = 873\ K$, $BLBR = 10\%$; (**b**) $T = 973\ K$, $BLBR = 10\%$; (**c**) $T = 1073\ K$, $BLBR = 10\%$; (**d**) $T = 1173\ K$, $BLBR = 10\%$; (**e**) $T = 1273\ K$, $BLBR = 10\%$.

According to Equation (10), there is a good linear relationship between $ln(k(T))$ and $1000/T$. The fitting results of five models are presented in Table 5: the kinetic parameters obtained under the five model functions are relatively close. According to the fitting linearity at different temperatures, the linear range, and the apparent activation energy calculated by the iso-conversional method, the F1 Model can better describe the bituminous coal combustion mechanism of the coupled combustion. The F1 Model achieved linear fitting within the range from 0.15 to 0.90 for carbon conversion, whereas the other models showed different linear fitting ranges. Based thereon, the activation energy and pre-exponential factor were estimated to be 45.45 kJ·mol^{-1} and 7.10 s^{-1}, respectively.

Table 5. Fitting results of mechanism function model (873–1273 K).

$G(\alpha)$	T	$k(T)$	R^2	α	E, A, R^2
F1	873 K	0.0147 s^{-1}	0.9530	0.15~0.92	E = 45.45 kJ·mol^{-1} A = 7.10 s^{-1} R^2 = 0.99
	973 K	0.0236 s^{-1}	0.9619	0.10~0.90	
	1073 K	0.0421 s^{-1}	0.9560	0.20~0.89	
	1173 K	0.0644 s^{-1}	0.9826	0.15~0.90	
	1273 K	0.1054 s^{-1}	0.9922	0.10~0.95	
R2	873 K	0.0049 s^{-1}	0.9088	0.10~0.89	E = 46.07 kJ·mol^{-1} A = 3.19 s^{-1} R^2 = 0.91
	973 K	0.0108 s^{-1}	0.9196	0.20~0.85	
	1073 K	0.0224 s^{-1}	0.9483	0.25~0.83	
	1173 K	0.0353 s^{-1}	0.9770	0.15~0.88	
	1273 K	0.0305 s^{-1}	0.9599	0.10~0.85	
R3	873 K	0.0047 s^{-1}	0.9253	0.10~0.89	E = 44.01 kJ·mol^{-1} A = 1.97 s^{-1} R^2 = 0.87
	973 K	0.0067 s^{-1}	0.9300	0.10~0.85	
	1073 K	0.0184 s^{-1}	0.9655	0.25~0.80	
	1173 K	0.0269 s^{-1}	0.9824	0.15~0.88	
	1273 K	0.0240 s^{-1}	0.9723	0.10~0.85	
F0	873 K	0.0066 s^{-1}	0.9662	0.05~0.99	E = 43.17 kJ·mol^{-1} A = 3.43 s^{-1} R^2 = 0.80
	973 K	0.0218 s^{-1}	0.9096	0.20~0.78	
	1073 K	0.0333 s^{-1}	0.9267	0.25~0.83	
	1173 K	0.0499 s^{-1}	0.9561	0.15~0.90	
	1273 K	0.0399 s^{-1}	0.9209	0.10~0.85	
A2	873 K	0.0111 s^{-1}	0.9837	0.10~0.94	E = 42.34 kJ·mol^{-1} A = 4.97 s^{-1} R^2 = 0.85
	973 K	0.0344 s^{-1}	0.9051	0.20~0.78	
	1073 K	0.0526 s^{-1}	0.9266	0.25~0.83	
	1173 K	0.0712 s^{-1}	0.9405	0.15~0.90	
	1273 K	0.0687 s^{-1}	0.9435	0.10~0.85	

3.2.3. The Effect of BLBR on the Kinetic Parameters

According to the concentration of CO and CO_2 gas production during the coupling combustion, the linear relationship of the integral function of the mechanism model function F1 Model versus the reaction time, t, under different BLBR is studied. The bituminous coal combustion mechanism can be described by the F1 Model at different BLBRs; the kinetic parameters are shown in Figure 8. According to Figure 8, the apparent activation energy of the F1 Model was 48.70, 46.75, and 42.35 kJ·mol^{-1}, and the pre-exponential factor was 9.26, 8.95, and 6.70 s^{-1} when the BLBR was 5, 20, and 30%, respectively. The bituminous coal combustion mechanism can be described by the F1 Model at different BLBRs, and the results of kinetic analysis are shown in Figure 8. According to Figure 8, when the BLBR is 5%, 20%, and 30%, respectively, the apparent activation energy is 48.70, 46.75, and 42.35 kJ·mol^{-1}, and the pre-exponential factor is 9.26, 8.95, and 6.70 s^{-1}. The results show that the apparent activation energy and the pre-exponential factor in coupled combustion changed slightly at different BLBRs. But, compared with bituminous coal combustion, the kinetic parameters of coupled combustion show a significant decrease [43]. Based on

the above results, it can be found that the coupled combustion significantly increases the reaction rate of bituminous coal combustion.

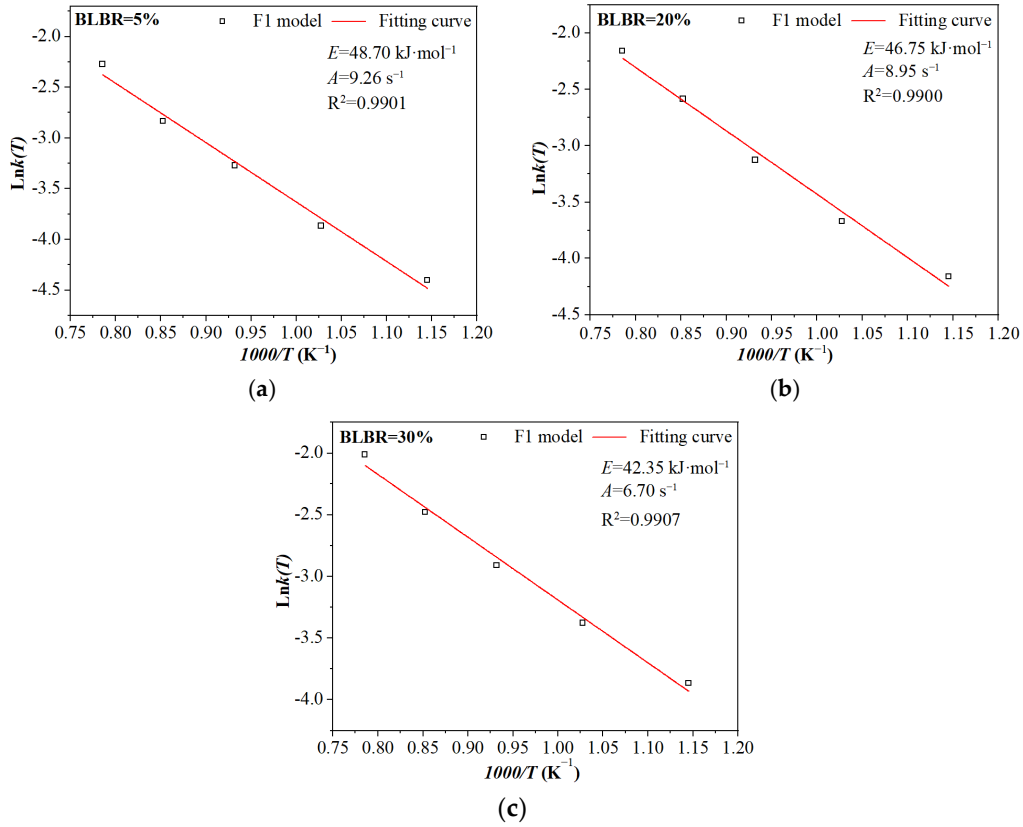


Figure 8. Linear fitting relationship diagram of $\ln k(T)$ and $1000/T$. (**a**) $T = 873 - 1273\ K,\ BLBR = 5\%$; (**b**) $T = 873 - 1273\ K,\ BLBR = 20\%$; (**c**) $T = 873 - 1273\ K,\ BLBR = 30\%$.

4. Conclusions

In this study, multiple sets of experiments on coupled combustion of bio-syngas and bituminous coal under different experimental conditions were carried out by a Micro-Fluidized Bed Reaction Analyzer (MFBRA). The concentrations of CO and CO_2 gas production were analyzed, and the influence of bio-syngas blending on the combustion characteristics of the coupled combustion were clarified, and the coupled combustion mechanism of bio-syngas and bituminous coal was revealed. The results indicate that the blending of bio-syngas significantly promotes the release of volatile fraction and improves the combustion reaction rate of bituminous coal, and the single peak trend of CO and CO_2 gas production release was found, so the ignition of bituminous coal in coupled combustion is a homogeneous ignition mechanism. The nucleation and growth model (F1 Model) can describe the kinetic mechanism of bituminous coal combustion reaction in coupled combustion. When the BLBR is 5, 10, 20, and 30%, the apparent activation energy obtained by F1 Model is 48.70, 45.45, 46.75, and 42.35 kJ·mol^{-1}, and the pre-exponential factor is 9.26, 7.10, 8.95, and 6.70 s^{-1}, respectively. The bio-syngas blending significantly reduces the apparent activation energy and pre-exponential factor of bituminous coal combustion reaction, but the bio-syngas lower heating value-based blending ratio (BLBR) has little effect on the kinetic parameters in coupled combustion. The revelation of the coupled combustion mechanism between bio-syngas and bituminous coal, along with the calculation of kinetic parameters, holds great significance for enhancing combustion efficiency, reducing emissions of gas Pollutant and ash, and optimizing the operation of combustion furnaces. It contributes to enhancing energy utilization efficiency, diminishing pollutant emissions, and providing valuable guidance for the design of combustion equipment. Looking ahead, further endeavors will be made to delve deeper into the detailed reaction mechanism. By

integrating high-performance computing and simulation technologies, a more comprehensive study of the coupled combustion process between bio-syngas and coal under diverse working conditions will be carried out.

Author Contributions: Conceptualization, A.H. and T.L.; methodology, Z.L. and B.G.; validation, A.H. and Z.L.; formal analysis, A.H. and B.G.; investigation, A.H. and Z.L.; writing—original draft, A.H., B.G. and Z.L.; writing—review and editing, T.L. and A.H(L). All authors have read and agreed to the published version of the manuscript.

Funding: This research was funded by Leading Goose Project of Qinghai Minzu University, grant number 23GCC21; and the APC was funded by Qinghai Minzu University, research grant no. 23GCC21 (project name: Research on integrated clean energy heating system in high-altitude agricultural and pastoral areas).

Data Availability Statement: The original contributions presented in the study are included in the article, further inquiries can be directed to the corresponding author.

Acknowledgments: The authors gratefully acknowledge the support provided by the laboratory members at Henan Key Lab of Biomass Energy for debugging of experiment system.

Conflicts of Interest: The authors declare no conflicts of interest.

References

1. Zhao, Y.; Su, Q.; Li, B.; Zhang, Y.; Wang, X.; Zhao, H.; Guo, S. Have Those Countries Declaring "Zero Carbon" or "Carbon Neutral" Climate Goals Achieved Carbon Emissions-Economic Growth Decoupling? *J. Clean. Prod.* **2022**, *363*, 132450. [CrossRef]
2. Mi, Z.; Meng, J.; Guan, D.; Shan, Y.; Song, M.; Wei, Y.-M.; Liu, Z.; Hubacek, K. Chinese CO_2 Emission Flows Have Reversed Since the Global Financial Crisis. *Nat. Commun.* **2017**, *8*, 1712. [CrossRef]
3. López, L.A.; Arce, G.; Jiang, X. Mapping China's Flows of Emissions in the World's Carbon Footprint: A Network Approach of Production Layers. *Energy Econ.* **2020**, *87*, 104739. [CrossRef]
4. Liu, Z.; Deng, Z.; He, G.; Wang, H.; Zhang, X.; Lin, J.; Qi, Y.; Liang, X. Challenges and Opportunities for Carbon Neutrality in China. *Nat. Rev. Earth Environ.* **2021**, *3*, 141–155. [CrossRef]
5. Kao, X.; Liu, Y.; Wang, W.; Wen, Q.; Zhang, P. The Pressure of Coal Consumption on China's Carbon Dioxide Emissions: A Spatial and Temporal Perspective. *Atmos. Pollut. Res.* **2024**, *15*, 102188. [CrossRef]
6. Gielen, D.; Boshell, F.; Saygin, D.; Bazilian, M.D.; Wagner, N.; Gorini, R. The Role of Renewable Energy in the Global Energy Transformation. *Energy Strategy Rev.* **2019**, *24*, 38–50. [CrossRef]
7. Tian, X.; An, C.; Chen, Z. The Role of Clean Energy in Achieving Decarbonization of Electricity Generation, Transportation, and Heating Sectors by 2050: A Meta-Analysis Review. *Renew. Sustain. Energy Rev.* **2023**, *182*, 113404. [CrossRef]
8. Tong, D.; Zhang, Q.; Liu, F.; Geng, G.; Zheng, Y.; Xue, T.; Hong, C.; Wu, R.; Qin, Y.; Zhao, H.; et al. Current Emissions and Future Mitigation Pathways of Coal-Fired Power Plants in China From 2010 to 2030. *Environ. Sci. Technol.* **2018**, *52*, 12905–12914. [CrossRef]
9. Liu, L.; Memon, M.Z.; Xie, Y.; Gao, S.; Guo, Y.; Dong, J.; Gao, Y.; Li, A.; Ji, G. Recent Advances of Research in Coal and Biomass Co-Firing for Electricity and Heat Generation. *Circ. Econ.* **2023**, *2*, 100063. [CrossRef]
10. Antar, M.; Lyu, D.; Nazari, M.; Shah, A.; Zhou, X.; Smith, D.L. Biomass for A Sustainable Bioeconomy: An Overview of World Biomass Production and Utilization. *Renew. Sustain. Energy Rev.* **2021**, *139*, 110691. [CrossRef]
11. Mishra, S.; Upadhyay, R.K. Review on Biomass Gasification: Gasifiers, Gasifying Mediums, and Operational Parameters. *Mater. Sci. Energy Technol.* **2021**, *4*, 329–340. [CrossRef]
12. Tezer, Ö.; Karabağ, N.; Öngen, A.; Çolpan, C.Ö.; Ayol, A. Biomass Gasification for Sustainable Energy Production: A Review. *Int. J. Hydrogen Energy* **2022**, *47*, 15419–15433. [CrossRef]
13. Mo, W.; Du, K.; Sun, Y.; Guo, M.; Zhou, C.; You, M.; Xu, J.; Jiang, L.; Wang, Y.; Su, S.; et al. Technical-Economic-Environmental Analysis of Biomass Direct and Indirect Co-Firing in Pulverized Coal Boiler in China. *J. Clean. Prod.* **2023**, *426*, 139119. [CrossRef]
14. Agbor, E.; Zhang, X.; Kumar, A. A Review of Biomass Co-Firing in North America. *Renew. Sustain. Energy Rev.* **2014**, *40*, 930–943. [CrossRef]
15. Dong, C.; Yang, Y.; Yang, R.; Zhang, J. Numerical Modeling of the Gasification Based Biomass Co-Firing in A 600MW Pulverized Coal Boiler. *Appl. Energy* **2010**, *87*, 2834–2838. [CrossRef]
16. Si, M.; Cheng, Q.; Yuan, L.; Zhang, Y.; Luo, Z. Study on the Combustion Behavior of Single Coal Particle Using a Thermal-Imaging Technique. *Combust. Flame* **2022**, *242*, 112178. [CrossRef]
17. Eaton, A.M.; Smoot, L.D.; Hill, S.C.; Eatough, C.N. Components, Formulations, Solutions, Evaluation, and Application of Comprehensive Combustion Models. *Prog. Energy Combust. Sci.* **1999**, *25*, 387–436. [CrossRef]
18. Wen, X.; Wang, H.; Luo, Y.; Luo, K.; Fan, J. Numerical Investigation of the Effects of Volatile Matter Composition and Chemical Reaction Mechanism on Pulverized Coal Combustion Characteristics. *Fuel* **2017**, *210*, 695–704. [CrossRef]

19. Guedea, I.; Pallarès, D.; Díez, L.I.; Johnsson, F. Conversion of Large Coal Particles Under O_2/N_2 and O_2/CO_2 Atmospheres—Experiments and Modeling. *Fuel Process. Technol.* **2013**, *112*, 118–128. [CrossRef]
20. Hecht, E.S.; Shaddix, C.R.; Geier, M.; Molina, A.; Haynes, B.S. Effect of CO_2 and Steam Gasification Reactions on the Oxy-Combustion of Pulverized Coal Char. *Combust. Flame* **2012**, *159*, 3437–3447. [CrossRef]
21. Bu, C.; Liu, D.; Chen, X.; Pallarès, D.; Gómez-Barea, A. Ignition Behavior of Single Coal Particle in A Fluidized Bed Under O_2/CO_2 and O_2/N_2 Atmospheres: A Combination of Visual Image and Particle Temperature. *Appl. Energy* **2014**, *115*, 301–308. [CrossRef]
22. Zhang, L.; Wu, D.; Cai, L.; Zou, C.; Qiu, J.; Zheng, C. The Chemical and Physical Effects of CO_2 on the Homogeneous and Heterogeneous Ignition of the Coal Particle in O_2/CO_2 Atmospheres. *Proc. Combust. Inst.* **2017**, *36*, 2113–2121. [CrossRef]
23. Lei, M.; Zou, C.; Xu, X.; Wang, C. Effect of CO_2 and H_2O on the Combustion Characteristics and Ash Formation of Pulverized Coal in Oxy-Fuel Conditions. *Appl. Therm. Eng.* **2018**, *133*, 308–315. [CrossRef]
24. Zhu, T.; Hu, Y.; Tang, C.; Wang, L.; Liu, X.; Deng, L.; Che, D. Experimental Study on NOx Formation and Burnout Characteristics of Pulverized Coal in Oxygen Enriched and Deep-Staging Combustion. *Fuel* **2020**, *272*, 117639. [CrossRef]
25. Fan, W.; Li, Y.; Guo, Q.; Chen, C.; Wang, Y. Coal-Nitrogen Release and NOx Evolution in the Oxidant-Staged Combustion of Coal. *Energy* **2017**, *125*, 417–426. [CrossRef]
26. Chen, X.; Zhang, C.; Chen, X.; Peng, Z.; Gao, H.; Gong, X. Performance Analysis of a Novel Biomass Gasification System Coupled to a Coal-Fired Power Plant Based on Heat and Water Recovery. *Energy Convers. Manag.* **2024**, *299*, 117822. [CrossRef]
27. Abid, S.; Zhang, X.; Zhang, W.; Mu, H.; Zhang, C.; Wang, A. System Performance and Pollution Emission of Biomass Gas Co-Firing in A Coal-Fired Boiler. *J. Power Energy Eng.* **2020**, *8*, 18–25. [CrossRef]
28. Ye, Y.L.; Wang, H.M.; An, X.; Jiang, W.H. Thermal Efficiency Calculating Model of Pulverized Coal and Blast Furnace Gas Co-Fired Boilers Based on Separate Combustion Calculation. *IOP Conf. Ser. Earth Environ. Sci.* **2018**, *186*, 012018. [CrossRef]
29. Han, Z.; Yue, J.; Zeng, X.; Yu, J.; Wang, F.; Sun, S.; Yao, H.; Luo, G.; Liu, X.; Sun, Y.; et al. Characteristics of Gas-Solid Micro Fluidized Beds for Thermochemical Reaction Analysis. *Carbon Resour. Convers.* **2020**, *3*, 203–218. [CrossRef]
30. Yu, J.; Zeng, X.; Zhang, J.; Zhong, M.; Zhang, G.; Wang, Y.; Xu, G. Isothermal Differential Characteristics of Gas–Solid Reaction in Micro-Fluidized Bed Reactor. *Fuel* **2013**, *103*, 29–36. [CrossRef]
31. Silva, J.; Teixeira, S.; Teixeira, J. A Review of Biomass Thermal Analysis, Kinetics and Product Distribution for Combustion Modeling: From the Micro to Macro Perspective. *Energies* **2023**, *16*, 6705. [CrossRef]
32. Wang, F.; Zeng, X.; Wang, Y.; Su, H.; Yu, J.; Xu, G. Non-Isothermal Coal Char Gasification with CO_2 in A Micro Fluidized Bed Reaction Analyzer and A Thermogravimetric Analyzer. *Fuel* **2016**, *164*, 403–409. [CrossRef]
33. Zhang, H.; Dou, B.; Li, J.; Zhao, L.; Wu, K. Thermogravimetric Kinetics on Catalytic Combustion of Bituminous Coal. *J. Energy Inst.* **2020**, *93*, 2526–2535. [CrossRef]
34. Aidabulov, M.; Zhakupov, D.; Zhunussova, K.; Temireyeva, A.; Shah, D.; Sarbassov, Y. Thermal Characterization, Kinetic Analysis and Co-Combustion of Sewage Sludge Coupled with High Ash Ekibastuz Coal. *Energies* **2023**, *16*, 6634. [CrossRef]
35. Tan, J.; He, Y.; Zhu, R.; Zhu, Y.; Wang, Z. Experimental Study on Co-Firing Characteristics of Ammonia with Pulverized Coal in A Staged Combustion Drop Tube Furnace. *Proc. Combust. Inst.* **2023**, *39*, 3217–3225. [CrossRef]
36. Zhang, K.; Wang, Z.; Fang, W.; He, Y.; Hsu, E.; Li, Q.; Gul-e-Rana, J.; Cen, K. High-Temperature Pyrolysis Behavior of A Bituminous Coal in A Drop Tube Furnace and Further Characterization of The Resultant Char. *J. Anal. Appl. Pyrol.* **2019**, *137*, 163–170. [CrossRef]
37. Balusamy, S.; Kamal, M.M.; Lowe, S.M.; Tian, B.; Gao, Y.; Hochgreb, S. Laser Diagnostics of Pulverized Coal Combustion in O_2/N_2 and O_2/CO_2 Conditions: Velocity And Scalar Field Measurements. *Exp. Fluids* **2015**, *56*, 108. [CrossRef]
38. Guo, Y.; Zhao, Y.; Gao, D.; Liu, P.; Meng, S.; Sun, S. Kinetics of Steam Gasification of In-Situ Chars in A Micro Fluidized Bed. *Int. J. Hydrogen Energy* **2016**, *41*, 15187–15198. [CrossRef]
39. Yu, J.; Yao, C.; Zeng, X.; Geng, S.; Dong, L.; Wang, Y.; Gao, S.; Xu, G. Biomass Pyrolysis in A Micro-Fluidized Bed Reactor: Characterization and Kinetics. *Chem. Eng. J.* **2011**, *168*, 839–847. [CrossRef]
40. Zaghib, K.; Song, X.; Kinoshita, K. Thermal Analysis of the Oxidation of Natural Graphite: Isothermal Kinetic Studies. *Thermochim. Acta* **2001**, *371*, 57–64. [CrossRef]
41. Vyazovkin, S.; Wight, C.A. Isothermal and Nonisothermal Reaction Kinetics in Solids: In Search of Ways Toward Consensus. *J. Phys. Chem. A* **1997**, *101*, 8279–8284. [CrossRef]
42. Vyazovkin, S.; Goryachko, V. Potentialities of Software for Kinetic Processing of Thermoanalytical Data by the Isoconversion Method. *Thermochim. Acta* **1992**, *194*, 221–230. [CrossRef]
43. He, A.; Li, Z.; Li, J.; Wang, X.; Zhang, L.; Yang, S.; Xin, X.; Sun, T.; Lei, T. Effects of Bio-Syngas Blends on Combustion Characteristics of Coal: Kinetic Analysis. *J. Biobased Mater. Bioenergy* **2021**, *15*, 269–277. [CrossRef]
44. Bai, W.; Li, H.; Deng, L.; Liu, H.; Che, D. Air-Staged Combustion Characteristics of Pulverized Coal under High Temperature and Strong Rreducing Atmosphere Conditions. *Energy Fuel* **2014**, *28*, 1820–1828. [CrossRef]

Disclaimer/Publisher's Note: The statements, opinions and data contained in all publications are solely those of the individual author(s) and contributor(s) and not of MDPI and/or the editor(s). MDPI and/or the editor(s) disclaim responsibility for any injury to people or property resulting from any ideas, methods, instructions or products referred to in the content.